Investigation to the contribution of cellular synovial fluid components for the infrared spectroscopic detection of equine osteoarthritis

Myrthe Barvelink
Student ID: 3586936
Master Equine Health
Faculty of Veterinary Medicine
Utrecht University
The Netherlands

Supervisors

Prof. Dr. C.B. Riley	Equine Research Centre, Equine Veterinary Clinic,
Dr. L. Panizzi	School of Veterinary Science, Massey University, New Zealand
Dr. H. Brommer	Department of Equine Sciences, Faculty of Veterinary Medicine, Utrecht University, The Netherlands

Table of contents

Abstract

Objective – To evaluate whether the ability of infrared spectroscopic methods to classify osteoarthritic and normal equine joints is improved by the removal of the cellular components of synovial fluid samples.

Method – Following approval from the Massey University Animal Ethics Committee, 16 untrained New Zealand Thoroughbred fillies (2 to 3 YO) were obtained. The horses were randomly allocated in two groups of eight animals (treatment and control). At day 0, arthroscopy was performed on one middle carpal joint of each treatment horse under general anaesthesia and an 8-mm osteochondral fragment was created ("Chip"), mimicking naturally occurring equine osteoarthritis (OA). The control horses underwent the same arthroscopic surgery, but no cartilage or subchondral bone damage was induced, serving as non-arthritic controls ("Sham"). Starting at day 14, horses were exercised on a high-speed treadmill for 5 consecutive days, followed by 2 days rest each week until the end of the study. Synovial fluid samples were collected weekly aseptically from both mid-carpal joints of each horse. From each sample, an aliquot was drawn (Neat) and the remaining fluid was centrifuged at 1000 g for 10 minutes, the supernatant was separated (Supernatant). For IR spectroscopy dry films were made for each sample and IR spectra were recorded in the mid-IR range. Briefly, principal component analysis (PCA) was performed after pre-processing the data and detecting outliers. Chip joints were compared with contralateral joints in the same horse and with sham joints. With each comparison, the optimal number of components were determined, and these found for neat and supernatant synovial fluids were compared by Wilcoxon matched pairs tests. Differences were considered significant for $p \leq 0.05$.

Results – Both the comparisons of the Chip joints versus the contralateral joints and the Chip joints versus the Sham joints showed that the percentage of explained variance was significantly higher for the analysis of neat synovial fluid spectra. Also, the neat samples showed good to moderate group separation in both comparisons while the supernatant samples showed poor group separation.

Conclusion and Clinical Relevance – The findings of this research seem to suggest that the cellular component of the synovial fluid does contribute in the development and diagnosis of OA. In order to create IR spectroscopic methods to detect OA, the model used in this study requires further development to improve it's diagnostic accuracy.

Introduction

With 68% of training days being lost due to lameness in cantering training, lameness is said to be the greatest cause of wastage among racehorses.[1] Several authors have found in their studies that lameness due to joint disease is the most significant factor responsible for inability to race and loss of performance.[1,2] Osteoarthritis (OA) is the most frequently seen (54% of all consulted orthopaedic cases in one hospital) cause of lameness in horses, and is thus a commonly encountered cause of impaired performance and welfare in horses.[3] OA compromises the equine industry not only because of impaired performance and welfare, but also because of the costs of the treatment of OA and the arsing financial consequences of a delayed return to athletic performance.[4] The condition affects horses of any age, but young racehorses are particularly at risk.[5] For example, as many as a third of assessed 2- to 3-year-old Thoroughbred racehorses have been found in one study to have partial or full-thickness cartilage lesions and OA in their metacarpophalangeal joints, based on macroscopic, histologic and biochemical analysis of cartilage.[5]

The triggers for the disease process that leads to OA may originate from various causes, with acute or repetitive trauma and concomitant synovitis accompanied by enzymatic tissue degradation being the most common in young horses.[6,7] This aetiology may be associated with conformational inadequacies that predispose athletic horses to excessive biomechanical forces on articular cartilage.[8,9] However, more usually it is associated with overuse, causing insidious damage due to multiple and cumulative repetitive traumatic insults, which can occur during the normal day to day athletic training of the horse.[3,9] The inflammatory process is most often started in the subchondral bone, joint capsule, cartilage or synovium, after which a cascade of inflammatory mediators is quickly initiated from the primary tissue insult.[9] Normally this inflammation would be counteracted by the homeostatic mechanisms within the synovial environment.[3] However, in situations where these mechanisms are insufficient to overcome and repair the tissue injury, or in situations where there are repeated traumatic insults, a 'domino effect' of the inflammatory process may extend into the adjacent joint tissues that initiates the release of additional inflammatory mediators.[3,9] The ongoing release of enzymes, inflammatory mediators and cytokines contribute to the progressive degradation and destruction of the articular cartilage.[3,6,9] When unimpeded, this cartilage degeneration, accompanied by subchondral bone sclerosis, osteophyte formation, varying degrees of

synovial inflammation and periarticular tissue fibrosis, makes OA a progressive and incurable disease.[3] Chronic OA is frequently associated with poor performance and chronic pain that varies in severity from mild and intermittent to severe and debilitating. Therefore, timely diagnosis and aggressive treatment are important to alleviate the effects of inflammation and are essential to prevent or minimize the development and progression of OA.[10]

The evaluation of joint disease in the horse is facilitated by a comprehensive clinical examination (including gait evaluation and localization with local anaesthesia), imaging modalities that include radiography, ultrasonography, computed tomography (CT), magnetic resonance imaging (MRI), nuclear medical imaging, arthroscopy and routine synovial fluid analysis.[11,12] The most common clinical findings include lameness, pain, synovial effusion, soft tissue swelling and a painful response to palpation and/or flexion.[3] Osteophytes, increased subchondral bone density and end-stage joint space reduction are the main radiological features of advanced OA.[7,13] However, the initial stages of OA are difficult to detect on radiographs, particularly if changes are limited to synovitis or mild to moderate cartilage injury without affecting the subchondral bone.[7] The interpretation of radiographs should be performed with caution, as there is no clear relationship between scores of radiographic findings and the degree of lameness presented by horses.[4] More advanced imaging modalities may provide more detailed information. Computed tomography (CT) offers some advantages with respect to the diagnosis of OA. It allows cross-sectional imaging of anatomic features and provides excellent detail of osseous structures with higher contrast resolution and diagnostic specificity than that achieved with radiography.[14] Several CT image characteristics, such as heterogeneous distribution of the subchondral bone and greater subchondral bone density appear to predict the presence of OA associated cartilage lesions in metacarpophalangeal joints of horses.[14] However, there is limited applicability for CT to visualization of the synovium and the synovial membrane. This is an important limitation, because synovitis is increasingly considered to be a key player in the OA disease process.[15] On low-field MRI, cartilage defects with various levels of signal change in the subchondral bone can be seen.[7] These lesions have a very high specificity for the detection of microscopic OA, but the sensitivity of this lesion category for microscopic OA seems to be low.[7,16] A more recent study used a semi-quantitative MRI whole-organ scoring system to characterize the progression of MRI changes in the middle carpal joint in an equine model of post-traumatic osteoarthritis.[17] The study results suggest

that changes in high- and low-signal bone lesions, osteophyte formation, subchondral bone irregularity, cartilage signal abnormalities, joint effusion and synovial thickening could be precisely scored with the MRI images, suggesting that this MRI scoring model might be useful in the identification and progression of pathological changes of equine OA.[17] Unfortunately, due to the costs of CT and MRI scans, the availability of these techniques are limited to larger practices, and imaging with these modalities is expensive.

As part of a push to develop economic and readily accessible approaches to early detection of OA, diagnostic approaches based on a more detailed understanding of disease markers and their interdependence are being pursued.[18–24] There have been a number of advances in the development of molecular, genetic and other serum and synovial fluid biomarkers assays for the prediction, early diagnosis and staging of musculoskeletal disease in performance horses.[18,19] However, with the exception of high end imaging biomarkers (MRI and CT), they have not generally been translated into routine clinical use.[20] The studies of Frisbie *et al*., 2008 and Bertuglia *et al*., 2016 proved that with the use of ELISA based assays several synovial fluid biomarkers and serum biomarkers can be of use for the early diagnosis of OA in horses in training.[21,22] Another radioimmunoassay-based report proved the existence of a correlation between concentrations of substance P (a pain mediator) and prostaglandin E_2 (an inflammatory mediator) in synovial fluid obtained from healthy and OA joints, where the median concentrations of both mediators were significantly increased in OA joints.[23] Equine-specific microarray analysis has also been used to identify genes from white blood cells that are differentially expressed in horses with experimentally induced OA, proving that several genes have the potential for use as a diagnostic aid for equine OA.[24] The above mentioned publications show that these different techniques for evaluating biomarkers for OA are promising for the early detection of OA, but all of these techniques require complex multiple assays, are sensitive to environmental conditions and operator error, and individual testing with these techniques is expensive.[25,26] Additionally, they all require reagents that must be properly stored as many are heat labile and only stable for a finite period of time.[27]

Fourier transform infrared spectroscopy (IR) is well established as a powerful quantitative and qualitative technique for diagnostic characterization of biological molecules in human and animal fluids and tissues.[28] When disease occurs within a living organism it affects key cellular

pathways in characteristic ways, and tissue and biofluid composition may be altered in a fashion characteristic of that disease.[25,28,29] This results in nuclear (e.g. DNA) and biomolecular changes that may be referred to as a "metabolic fingerprint" of that disease.[25,28,29] Such information can be captured directly as an IR spectroscopic spectrum.[25,28,29] As demonstrated by research on human synovial fluids, IR spectroscopy can be of use in diagnosing joint disease and potentially differentiating between various joint diseases.[25,30] Studies performed on equine synovial fluid have demonstrated that the IR spectroscopic patterns of fluid from joints with traumatic OA differ significantly from the corresponding patterns for controls, and the spectra of joints with osteochondrosis deviate significantly from those derived from healthy control joints.[31,32] IR spectroscopy has been shown to be a sufficiently sensitive technique to differentiate between the synovial fluid from anatomically different but normal joints within horses.[27] More recently, studies in rabbits with an acute osteoarthritis model showed that the IR biomarker signature was different between the early inflammatory phase of traumatic osteoarthritis, and the transition to chronic joint disease.[33]

In most studies of synovial fluid biomarkers to date, IR spectroscopy is performed on films made from the synovial fluid without molecular separation or fractionation.[25,30–32] However, cytology changes may also be valuable in the assessment of synovial fluid.[34,35] Several studies on human cells including lymphocytic leukaemia cells, leukocytes, fibroblasts and cells found in human urine have proven the usefulness of cellular IR spectroscopy independent of the liquid component of these biofluids.[36–40] Although some progress has been made in the use of unprocessed "neat" synovial fluid for the IR spectroscopic identification of joint disease, to the author's knowledge there has been no investigation to determine whether it is the cellular or extracellular biomolecular components within the fluid that are of the greatest diagnostic importance. Additionally, there have recently been attempts to improve the ability of IR spectroscopy to detect changes within serum and plasma by subjecting them to various pre-processing approaches.[41]

Study Objectives

The overall objective of this study was to develop more accurate IR spectroscopic methods, using synovial fluid from horses with traumatically induced OA and controls. More specifically the aim of this study is to evaluate whether the ability of this technique to classify diseased

and normal joints is improved by the removal of the cellular components of synovial fluid samples. It was hypothesized that the spectra of synovial fluid from joints developing OA will differ from the spectra of the healthy joints, and that the depletion of cellular components recovered from the fluid will enhance the accuracy of this IR -based assay as a classification tool for OA.

Research Design and Methods

Animals

Following approval from the Massey University Animal Ethics Committee, 16 New Zealand bred, raised and unraced Thoroughbred fillies (2 to 3 YO) were obtained. Inclusion criteria were absence of lameness, absence of clinical abnormalities of all palpable joints, and absence of radiographic abnormalities of the carpal joints.

Procedures

The study horses were randomly allocated in two groups of eight animals (treatment and control). Prior to the start of the protocol, horses were acclimatised to the research environment and the treadmill (2 minutes trotting followed by 2 minutes canter and 2 minutes trotting) for 10-14 days. Arthroscopy was performed on one middle carpal joint of each treatment ("Chip") horse under general anaesthesia (day 0) using standard arthroscopic techniques as described by McIlwraith *et al*., 2015.[42] Specifically, in eight horses an 8-mm osteochondral fragment was created with an orthopaedic hammer and an 8 mm curved osteotome on the distal radial carpal bone, and the exposed subchondral bone between the fragment and parent bone was debrided to form a 15 mm wide defect. The size, location of the fragment, loss of bone, and subsequent synovitis mimic naturally occurring equine OA.[22,43,44] In the remaining eight horses one middle carpal joint was arthroscopically explored using the same surgical approach, but no cartilage or subchondral bone damage was induced; these horses served as non-arthritic controls ("Sham") .[43–45] Horses were housed in stalls, and the bandages were changed every 2-3 days as needed until suture removal. Phenylbutazone was administered orally (4.4 mg/kg SID) for 4 days post-operatively. The sutures were removed on day 10. Starting at day 14, horses were exercised on a high-speed treadmill for 5 consecutive days each week until the end of the study; the horses were rested for 2 days between each 5-day exercise period. Exercise of the horses included trotting (~18 km/h) for 2 minutes, galloping (~ 32 km/h) for 2 minutes, and trotting again (~18 km/h) for 2 minutes to simulate race-training exercise.

Samples

Synovial fluid samples were collected aseptically from both mid-carpal joints of each horse at days 0, 7, 14, 21, 28, 35, 42, 49, 56, and 63. This resulted in four different sets of samples: "Chip joint" and "Chip control" (contralateral joint) synovial fluid samples from the "Chip" horses, and; "Sham joint" and "Sham control" from the "Sham" operated horses. Each sample was divided and aliquots were placed into an EDTA containing tube for routine synovial fluid analysis (total protein concentration, cytologic evaluation, and total white blood cell count), an EDTA containing tube for later formalin fixation, and into a cryovial stored at –80°C for later IR biochemical marker evaluation.[31]

Sample preparation for infrared spectroscopy

Synovial fluid samples from the cryovials were processed prior to IR evaluation. A 100 µL aliquot of synovial fluid was removed from the samples into an Eppendorf vial as a neat sample. This neat sample was stored at -80°C for later IR spectroscopy. The remaining fluid was centrifuged at 1000 g for 10 minutes. After centrifugation the supernatant was separated from the pellet into a vial by careful aspiration using a pipette. The supernatant samples were stored at -80°C for later IR spectroscopy.

Infrared spectroscopy

All neat and supernatant synovial fluid samples were thawed for one hour to room temperature (20-22°C). Samples were prepared as described previously with the following modification.[46] For each sample, an aliquot was drawn and diluted in sterile water in a ratio 3: 1 (synovial fluid : water). Triplicate dry films were made for each sample by applying 8 µL of the diluted synovial fluid, spread evenly in a circular motion, onto 5-mm-diameter circular islands within a custom made, adhesive masked, silicon microplate. The adhesive mask served to spatially define and systematically separate the 5-mm islands on the microplate so that sample islands were correctly aligned with the IR detector window. Synovial films were left to dry at 20-22°C for 12 hours in a vacuum chamber to remove water. After the films were thoroughly dried, the microplate was mounted in a multisampler interfaced to the IR spectrometer to enable acquisition of infrared spectra. Infrared spectroscopic measurements of all samples were performed during the same period. Infrared spectra in the mid-infrared

range of 400 to 4,000 cm^{-1} were recorded with an IR spectrometer equipped with a deuterium tryglycine sulfate detector. For each acquisition, 512 interferograms was signal averaged and Fourier transformed to generate a spectrum with a nominal resolution of 4 cm^{-1}.

Data pre-processing and statistical analysis

For IR data analysis, chemometric techniques were used to model IR data over time and between groups in Unscrambler® X (Version 10.5 from CAMO, Oslo, Norway). Two sets of analyses were performed. The first set of analyses sought to classify synovial fluid from the Chip joints in comparison with Sham joint samples (CS). The second set of analyses sought to classify Ship joint comparison with Chip control joint (ChC) samples (i.e. within horses). For each set of analyses, spectroscopic data generated from the synovial samples (neat and supernatant separately) was plotted in Unscrambler X. Various iterative strategies for pre-processing of the data were compared to optimise the classification of the data including the evaluation of the first order and second order differential spectra, and smoothing of the data using Savitsky-Golay numerical algorithms (7, 9, 11, 13 and 15 point smoothing were compared). These approaches were used to resolve overlapping signals, enhance signal properties, and suppress unwanted spectral features that arise due to non-ideal instrument and sample properties. Single normal variate transformation (SNV), a mathematical correction of the spectra to increase the distinction between desired information and physical interference by reducing or multiplicative interference, was then performed. In SNV, each spectrum was transformed by subtracting the spectrum mean and scaled (divided) by the spectrum standard deviation.[47] For each pre-processed group of spectra (e.g. second order derivatives with 11 point smoothing), principal component analysis (PCA) with mean centring was performed for each sampling day.[47] All wave number variables were given an equal unitary weighting and the singular value decomposition (SVD) algorithm selected. Because the number of observations per day was limited, full leave-one-out cross validation was performed to create validation output. A Hotelling's T^2 plot was used for outlier detection with default p value set at 0.05. Where significant outliers were detected, these data were omitted from the dataset, and PCA repeated. The results of these analyses describing the explained variation by the optimized number of principal components, and showing synovial fluid group separation by post-operative day are given in the results section.

With each comparison (i.e. Chip vs ChC, and Chip vs CS), the optimal number of components found for neat and supernatant (cell free) synovial fluids were compared by Wilcoxon matched pairs tests. Differences were considered significant for $p \leq 0.05$.

Results

The outcomes of the IR data analysis are shown in Appendix 1 for the chip joint versus the contralateral control joint and in Appendix 2 for the chip joint versus the sham joint.

Chip horses: chip joint versus contralateral control joint

Following the Wilcoxon matched pairs test, there was no significant difference in the number of optimal components detected between neat and supernatant fluids. The percentage of explained variance was significantly higher for the analyses of neat synovial fluid spectra for both the optimal number ($p = 0.028$) of components and for 20 principal components ($p = 0.008$). The neat samples show good group separation between the chip joint and the contralateral joint on days 7 and 28, and moderate group separation on day 14, 21, and 35, while the supernatant samples did not show clear group separation at all.

Chip horse versus sham horse: chip joint versus sham joint

Following the Wilcoxon matched pairs test, there was no significant difference in the number of optimal components detected between neat and supernatant fluids. The percentage of explained variance was significantly higher for the analyses of neat synovial fluid spectra for both the optimal number ($p = 0.021$) of components and for 20 principal components ($p = 0.021$). The neat samples show good group separation between the chip joint and the contralateral joint on day 14, and moderate group separation on day 7, 21, 49, while the supernatant samples only show moderate group separation on day 35, 42 and 49.

Discussion

The results of this report show that with PCA from the spectra of the synovial fluids often differences are found between the joints with the osteochondral fragment, which mimic naturally occurring equine OA, and the control joints. This differentiation was visible when the chip joints were compared with the contralateral control joints and with the sham operated joints. It is notable that when the OA joint is compared with the contralateral joint in the same horse, the neat samples show good to moderate group separation while the supernatant samples show hardly any group separation. This suggests that cell containing fraction of synovial fluid is of importance in discriminating between OA and control joints by IR spectroscopy. Also, for both the comparisons of the chip joints versus the contralateral control joints and the chip joints versus the sham operated joints, the percentages of explained variance were significantly higher for the analyses of neat synovial fluid spectra for both the optimal number of components and for 20 principal components. These lower percentages of explained variances for the supernatant samples show some loss of important information, since the model that is made by the PCA analysis is apparently less precise for these samples. These findings seem to suggest that the cellular and other precipitated components of the synovial fluid do contribute in the IR-based development and diagnosis of OA. Further investigation is required to determine if the cellular components are the key to IR spectroscopic separation of OA and control joints, or if it is the combination of cellular and soluble markers that improves diagnostic discrimination.

Unfortunately, inflammatory cells in equine OA synovial fluid have rarely been studied. Generally, it is stated that the total and differential white cell counts in synovial fluid of human joints provide an easy way of differentiating inflammatory from non-inflammatory arthritides.[34] Also, the percentage of polymorphonuclear cells has been reported to be a good guide to the degree of joint inflammation.[34] However, the validity of both of these statements are barely assessed, making diagnosing OA based on SF inspection and cell counts quite unreliable.[34] Freemont *et al.,* 1991 states that normal synovial fluid of healthy human joints contains very few cells.[48] In healthy synovial fluid, two innate cell types are found, these are identical to the two types of synoviocytes which are found at the transition between the synovium and the synovial fluid.[48] The one group consists of synthetic cells which produce important constituents of the synovial fluid, the other group of cells are phagocytic.[48] As a

result, these cells help to maintain the structural and chemical integrity of the synovial fluid.[48] Normal synovial fluid also contains migratory cells of the immune system such as lymphocytes and macrophages.[48] When joint disease occurs, the total number of cells in the synovial fluid will increase, however, the concentration of cells may not always change significantly because the volume of the joint fluid can increase proportionally as well.[48] In inflammatory joint disease, the total cell number can increase dramatically, and marked changes occur in the proportions of the various cell types with a very marked increase in the number of leucocytes derived from the blood.[48] Non-inflammatory arthropathies, like OA, are marked by an increase of synoviocyte-like cells and either have synovial fluid nucleated cell counts of less than 10^9/l or between 10^9 and 1-5 x 10^9 cells/l with a predominance of lymphocytes or large mononuclear cells or both.[48,49] Only in osteoarthritis more than 50% of the nucleated cells are synoviocytes.[49] Unfortunately, these values are only described by Freemont *et al*., 1991, and the reliability of these values has not been widely discussed and reported.

Which specific cell types are involved in the synovial reactions of these joints is hard to say from the spectroscopic data only. The results of this paper should then be compared with the cytological findings of the synovial analysis. It is remarkable that the results mainly show group separation in the first weeks of the study (Chip vs contralateral control: days 7, 14, 21, 28 and 35 and Chip vs Sham: days 7, 14, 21, 49). Since it is unclear which specific cell types are involved in the synovial reactions it cannot be excluded that the joints may have been acutely inflamed after the surgery. This acute inflammation could be associated with surgical trauma and synovitis. The cause for this group separation in the first weeks of the study might also be caused by the non-inflammatory reaction caused by the used equine OA model written by McIlwraith *et al*., 2012.[7] In the supernatant group no group separation is visible in the first weeks, which makes inflammation in the joints due to surgery less likely. However, in case of inflammation due to surgery, it would have been expected that group separation would also be visible in the later weeks of this study, since in case of OA, the joints would not heal. The later inflammation would then have reflected ongoing chronic synovitis plus contributions from cartilage degeneration and bony remodeling. With the information given, the author can not explain the cause of this loss of group separation in the last weeks of the study. To find a cause, it would be necessary to compare these findings with the cytological finding of the synovial analysis.

Although most studies about IR spectroscopy of synovial fluid biomarkers are carried out only on the supernatants of the synovial fluid, the results above show that cytology changes are valuable as well in the assessment of synovial fluid of OA joints.[25,30,31,33] In the IR analysis of the supernatants of the joint fluids in this study, no group separation was found with the expectation of moderate group separation on days 35, 42 and 49 in the comparison of the Chip joints vs the Sham joints. This is remarkable, considering that previous IR studies on synovial fluid of OA joints did find differences between the spectra of OA joints and control joints.[25,30,31,33] The methods by which the samples were treated in this research are equal to the methods used by the other studies.[31,33] However, the method of pre-processing the IR spectra and the statistical analysis used in this study are not the same as the methods used in the previous studies.[31,33] This suggests that the methods used in this study may possibly be more suitable for analyzing cytological changes than analyzing biochemical changes in the supernatant of OA joints.

The results of this study seem to suggest that cellular components in the synovial fluid from OA joints play a role in the development and marker responses of OA and that they might be useful in the detection of OA in equine joints. The author believes that the principal component analysis used for this paper was sufficient to give an answer to the current research question. However, this model needs further adjustments to provide more robust interpretable results. The model used now finds the best principal components for each individual sample. This way, the principal components can differ a lot between samples what makes comparing the PCA results of the different samples subjective. It would be interesting to find out if there is a connection between the principal components of the different samples. Principal components that reflect cytological changes in the neat samples would then not be found in the PCA's of the supernatant samples, serving as a control for this study. Also, with this improved model, it might be possible to develop an accurate IR spectroscopic method that could be useful to diagnose OA in synovial fluid from horses.

Conclusions

In this study, we have shown that IR spectroscopy of non-cell depleted synovial fluid can be promising in the diagnosis of OA and the monitoring of its progression. The findings of this research seem to suggest that the cellular component of the synovial fluid does contribute in the development and diagnosis of OA. The opposite of what was expected was found in this study, since OA joints could be separated from control joints based on IR spectroscopy on non-cell-depleted synovial fluid, while no to only very little separation was found in the analysis of the supernatants of the synovial fluids of the joints. Therefore, it can be concluded from this study that depletion of cellular components recovered from the synovial fluid does not enhance the accuracy of this IR-based assay as a classification tool for OA. However, in order to create IR spectroscopic methods to detect OA, the model used in this study needs further adjustments to give more diagnositically accurate results.

Acknowledgements

I would like to express my appreciation to Prof. Dr. Chris Riley for giving me the opportunity to fulfil my research at the equine research centre at Massey University. Thank you very much for your hospitality, for sharing your knowledge with me, and for your patience explaining me and helping me with the spectroscopic data. You gave me the opportunity to really understand every aspect of my research. Also thank you and your family for making me feel so much at home in Palmerston North.

Another person I would like to thank for helping me during my stay at Massey University is Dr. Luca Panizzi. Thank you for letting me be a part of your research group and for collecting all the synovial samples for my project. I have learned a lot from you and had a great time working with you.

Of course my research internship would not exist without the help and support from Utrecht University from Dr. Harold Brommer. Thank you for your help and support while writing my paper and for your quick responses to my questions.

At last I would like to thank everyone involved in my research at Massey University. Marty Johnson for the endless good conversations every day while training our horses, Karen Dittmer for helping me with all the lab work, Dr. Bob Colborne for giving me the opportunity to be involved with other studies in our horses, Rachel Holcroft for taking such good care of the horses and helping me organise my samples, and thank you to all the others for the help and the awesome experience. I had an unforgettable time in Palmy!

References

1. Rossdale, P. D., Hopes, R., Digby, N. J. W. & Offord, K. Epidemiological study of wastage among racehorses 1982 and 1983. *Vet. Rec.* 116, 66–69. 1 ref (1985).
2. JEFFCOTT, L. B., ROSSDALE, P. D., FREESTONE, J., FRANK, C. J. & TOWERS-CLARK, P. F. An assessment of wastage in Thoroughbred racing from conception to 4 years of age. *Equine Vet. J.* 14, 185–198 (1982).
3. Kidd, J. A., Fuller, C. & Barr, A. R. S. Osteoarthritis in the horse. *Equine Vet. Educ.* 13, 160–168 (2001).
4. Souza, M. V. de. Osteoarthritis in horses – Part 1 : relationship between clinical and radiographic examination for the diagnosis. *Brazilian Arch. Biol. Technol.* 59, 1–9 (2016).
5. H. Neundorf, R. *et al.* Determination of the prevalence and severity of metacarpophalangeal joint osteoarthritis in Thoroughbred racehorses via quantitative macroscopic evaluation. *Am. J. Vet. Res.* 71, 1284–1293 (2010).
6. McIlwraith, C. W. Joint Disease in the Horse. in *General pathobiology of the joint and response to injury* 40–70 (1996).
7. McIlwraith, C. W., Frisbie, D. D. & Kawcak, C. E. The horse as a model of naturally occurring osteoarthritis. *Bone Jt. Res.* 1, 297–309 (2012).
8. E Schlueter, A. & Orth, M. Equine osteoarthritis: a brief review of the disease and its causes. *Equine Comp. Exerc. Physiol.* 1, 221–231 (2004).
9. Goodrich, L. R. & Nixon, A. J. Medical treatment of osteoarthritis in the horse – A review. *Vet. J.* 171, 51–69 (2006).
10. McIlwraith, C. W. Diseases of joints, tendons, ligaments, and related structures. in *Adams'lameness in horses* 459–644 (Lippincott Williams & Wilkins, 2002).
11. Park, R. D., Wrigley, R. H. & Steyn, P. F. Equine diagnostic imaging. in *Adams' lameness in horses* 185–375 (Lippincott Williams & Wilkins, 2002).
12. Pelt. Interpretation of synovial fluid findings in the horse. *J. Am. Vet. Med. Assoc.* 165, 91–95 (1974).
13. Hayashi, D., Roemer, F. W. & Guermazi, A. Imaging for osteoarthritis. *Ann. Phys. Rehabil. Med.* 59, 161–169 (2016).
14. Young, B. D., Samii, V. F., Mattoon, J. S., Weisbrode, S. E. & Bertone, A. L. Subchondral bone density and cartilage degeneration patterns in osteoarthritic metacarpal condyles of horses. *Am. J. Vet. Res.* 68, 841–849 (2007).
15. Braun, H. J. & Gold, G. E. Diagnosis of Osteoarthritis: Imaging. *Bone* 51, 278–288 (2012).
16. Ley, C. J., Björnsdóttir, S., Ekman, S., Boyde, A. & Hansson, K. Detection of early

osteoarthritis in the centrodistal joints of Icelandic horses: Evaluation of radiography and low-field magnetic resonance imaging. *Equine Vet. J.* 48, 57–64 (2016).

17. Smith, A. D. *et al.* Magnetic Resonance Imaging Scoring Of An Experimental Model Of Post-Traumatic Osteoarthritis In The Equine Carpus. *Vet. Radiol. Ultrasound* 57, 502–514 (2016).
18. Laverty, S. What biomarkers are telling us and the challenges ahead. *Havemeyer Found. Monogr. Ser.* 14–15. (2008).
19. McIlwraith, C. W. Use of synovial fluid and serum biomarkers in equine bone and joint disease: a review. *Equine Vet. J.* 37, 473–482. (2005).
20. Weeren, P. R. van & Firth, E. C. Future tools for early diagnosis and monitoring of musculoskeletal injury: biomarkers and CT. *Vet. Clin. North Am. Equine Pract.* 24, 153–175. (2008).
21. Bertuglia, A., Pagliara, E., Grego, E., Ricci, A. & Brkljaca-Bottegaro, N. Pro-inflammatory cytokines and structural biomarkers are effective to categorize osteoarthritis phenotype and progression in Standardbred racehorses over five years of racing career. *BMC Vet. Res.* 12, 246 (2016).
22. Frisbie, D. D., Al-Sobayil, F., Billinghurst, R. C., Kawcak, C. E. & McIlwraith, C. W. Changes in synovial fluid and serum biomarkers with exercise and early osteoarthritis in horses. *Osteoarthr. Cartil.* 16, 1196–1204 (2008).
23. KirkerHead, C. A. *et al.* Concentrations of substance P and prostaglandin E2 in synovial fluid of normal and abnormal joints of horses. *Am. J. Vet. Res.* 61, 714–718. 42 ref (2000).
24. Kamm, J. L., Frisbie, D. D., McIlwraith, C. W. & Orr, K. E. Gene biomarkers in peripheral white blood cells of horses with experimentally induced osteoarthritis. *Am. J. Vet. Res.* 74, 115–121 (2013).
25. Shaw, R. A. *et al.* Arthritis diagnosis based upon the near-infrared spectrum of synovial fluid. *Rheumatol. Int.* 15, 159–165 (1995).
26. McIlwraith, C. W., Billinghurst, R. C. & Frisbie, D. D. Current and future diagnostic means to better characterize osteoarthritis in the horse - routine synovial fluid analysys and synovial fluid and serum markers. in *American Association Equine Practice* 47, 171–179 (2001).
27. Riley, C., Hou, S., Vijarnsorn, M. & Shaw, A. Biochemical Variation Among Normal Equine Carpal and Tarsocrural Joint Fluids are Detected by Infrared Spectral Characteristics and A Modified Approach to Linear Discriminant Analysis. *GSTF Journal*

of Veterinary Science 1, (2014).

28. Shaw, R. A. & Mantsch, H. H. Infrared Spectroscopy of Biological Fluids in Clinical and Diagnostic Analysis. in *Encyclopedia of Analytical Chemistry* 83–102 (John Wiley & Sons, Ltd, 2000).
29. Wang, L. & Mizaikoff, B. Application of multivariate data-analysis techniques to biomedical diagnostics based on mid-infrared spectroscopy. *Anal. Bioanal. Chem.* 391, 1641–1654 (2008).
30. Eysel, H. H. *et al.* A novel diagnostic test for arthritis: Multivariate analysis of infrared spectra of synovial fluid. *Biospectroscopy* 3, 161–167 (1997).
31. Vijarnsorn, M. *et al.* Use of infrared spectroscopy for diagnosis of traumatic arthritis in horses. *Am. J. Vet. Res.* 67, 1286–1292. 42 ref (2006).
32. Vijarnsorn, M., Riley, C. B., Ryan, D. A., Rose, P. L. & Shaw, R. A. Identification of infrared absorption spectral characteristics of synovial fluid of horses with osteochondrosis of the tarsocrural joint. *Am. J. Vet. Res.* 68, 517–523 (2007).
33. Riley, C., Laverty, S., Hou, S. & Shaw, R. Infrared-based detection of an osteoarthritis biomarker signature in the serum of rabbits with induced osteoarthritis. in *Osteoarthritis and Cartilage 23* (2015).
34. Swan, A., Amer, H. & Dieppe, P. The value of synovial fluid assays in the diagnosis of joint disease: a literature survey. *Ann. Rheum. Dis.* 61, 493–498 (2002).
35. El-Gabalawy, H. S. Synovial fluid analysis, synovial biopsy, and synovial pathology. in *Kelley's Textbook of Rheumatology* 753–769 (Saunders, 2013).
36. Schultz, C. P., Liu, K.-Z., Johnston, J. B. & Mantsch, H. H. Prognosis of chronic lymphocytic leukemia from infrared spectra of lymphocytes. *Mol. Spectrosc. Mol. Struct. 1996* 408–409, 253–256 (1997).
37. Schultz, C. P., Liu, K., Johnston, J. B. & Mantsch, H. H. Study of chronic lymphocytic leukemia cells by FT-IR spectroscopy and cluster analysis. *Leuk. Res.* 20, 649–655 (1996).
38. Liu, K. Z., Xu, M. & Scott, D. A. Biomolecular characterisation of leucocytes by infrared spectroscopy. *Br. J. Haematol.* 136, 713–722 (2007).
39. Pacifico, A., Chiriboga, L. A., Lasch, P. & Diem, M. Infrared spectroscopy of cultured cells: II. Spectra of exponentially growing, serum-deprived and confluent cells. *A Collect. Pap. Present. Shedding New Light Dis. Opt. Diagnostics New Millenn. (SPEC 2002) Reims, Fr. 23-27 June 2002* 32, 107–115 (2003).
40. Bird, B. *et al.* Cytology by Infrared Micro-Spectroscopy: Automatic Distinction of Cell Types in Urinary Cytology. *Vib. Spectrosc.* 48, 101–106 (2008).

41. Elsohaby, I. *et al.* Centrifugal ultrafiltration of human serum for improving immunoglobulin A quantification using attenuated total reflectance infrared spectroscopy. *J. Pharm. Biomed. Anal.* 150, 413–419 (2018).
42. McIlwraith, C. W., Nixon, A. J. & Wright, I. M. Diagnostic and Surgical Arthroscopy of the Carpal Joint. in *Diagnostic and Surgical Arthroscopy in the Horse* 45–110 (2015).
43. Kawcak, C. E., Frisbie, D. D., Werpy, N. M., Park, R. D. & McIlwraith, C. W. Effects of exercise vs experimental osteoarthritis on imaging outcomes. *Osteoarthr. Cartil.* 16, 1519–1525 (2008).
44. Frisbie, D. D., Ghivizzani, S. C., Robbins, P. D., Evans, C. H. & McIlwraith, C. W. Treatment of experimental equine osteoarthritis by in vivo delivery of the equine interleukin-1 receptor antagonist gene. *Gene Ther.* 9, 12 (2002).
45. Frisbie, D. D. *et al.* Serum biomarker levels for musculoskeletal disease in two- and three-year-old racing Thoroughbred horses: a prospective study of 130 horses. *Equine Vet. J.* 42, 643–651. 43 ref (2010).
46. Shaw, R. A. & Mantsch, H. H. Multianalyte serum assays from mid-IR spectra of dry films on glass slydes. *Appl. Spectrosc.* 54, 885–889 (2000).
47. Chalmers, J. M., Edwards, H. G. M. & Hargreaves, M. D. Vibrational Spectroscopy Techniques: Basics and Instrumentation. in *Infrared and Raman Spectroscopy in Forensic Science* 9–44 (John Wiley & Sons, 2012). doi:10.1002/9781119962328.ch2
48. Freemont, A. J. Role of cytological analysis of synovial fluid in diagnosis and research. *Ann. Rheum. Dis.* 50, 120–123 (1991).
49. Freemont, A. J., Denton, J., Chuck, A., Holt, P. J. & Davies, M. Diagnostic value of synovial fluid microscopy: a reassessment and rationalisation. *Ann. Rheum. Dis.* 50, 101 LP-107 (1991).

Appendix 1. Chip vs. ChipControl

Results – PCA based classification of synovial fluid samples from horses with an experimentally induced radiocarpal bone fracture versus within horse contralateral controls

Day 0 (preoperative)

Neat synovial fluid

Scores plot of first and second PCA components following outlier removal

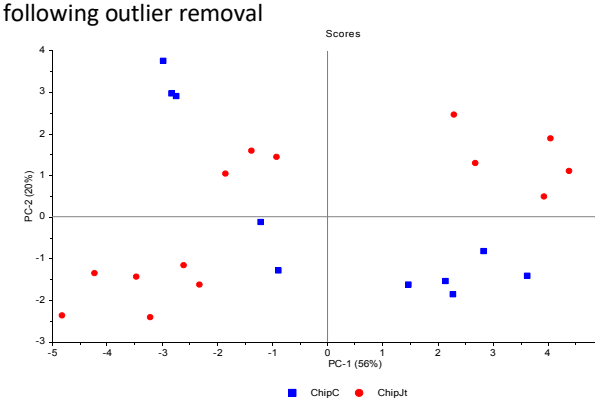

Supernatant of processed synovial fluid

Scores plot of first and second PCA components following outlier removal

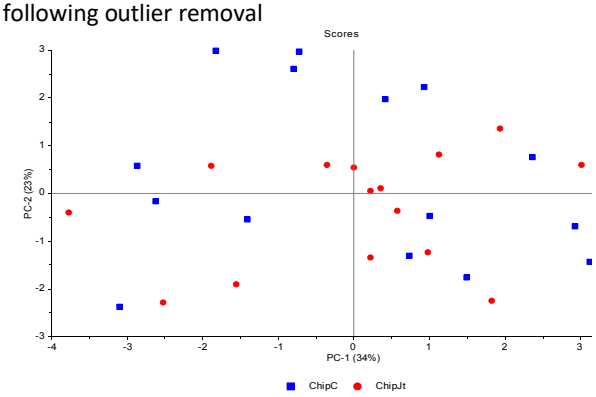

Optimal number of components	Four	Optimal number of components	Five
Explained variance with optimal number of components			
Calibration (%)	91.6	Calibration (%)	88.4
Validation (%)	87.7	Validation (%)	82.2
Explained variance with 20 components			
Calibration (%)	99.6	Calibration (%)	98.3
Validation (%)	92.4	Validation (%)	86.8

Day 7

Neat synovial fluid

Scores plot of first and second PCA components following outlier removal

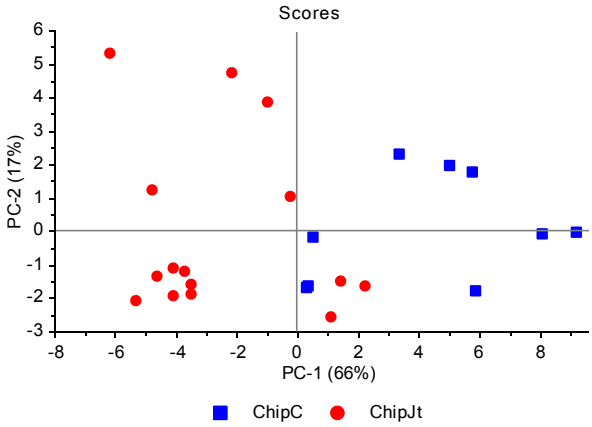

Supernatant of processed synovial fluid

Scores plot of first and second PCA components following outlier removal

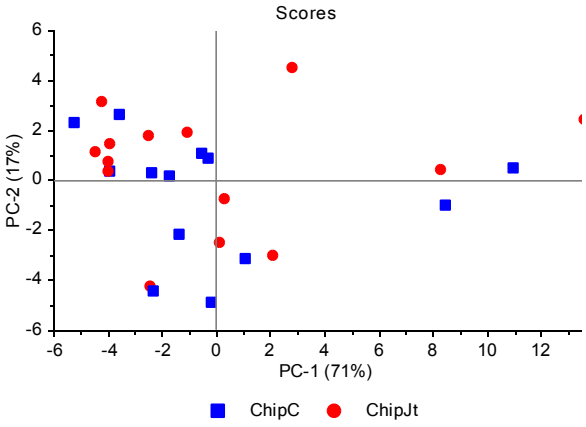

Optimal number of components	Four	Optimal number of components	Four
Explained variance with optimal number of components			
Calibration (%)	93.7	Calibration (%)	94.9
Validation (%)	90.0	Validation (%)	91.9
Explained variance with 20 components			
Calibration (%)	99.8	Calibration (%)	99.6
Validation (%)	93.4	Validation (%)	94.7

Day 14

Neat synovial fluid

Scores plot of first and second PCA components following outlier removal

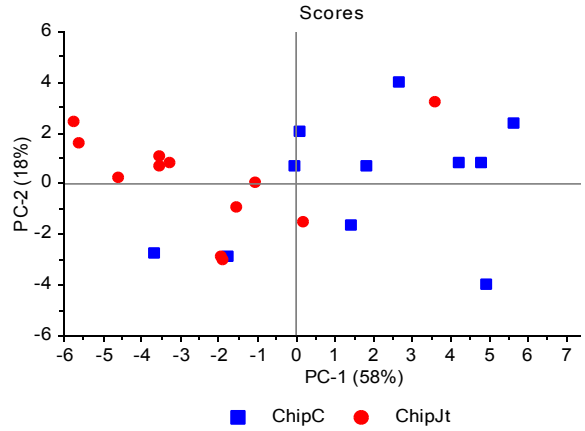

Supernatant of processed synovial fluid

Scores plot of first and second PCA components following outlier removal

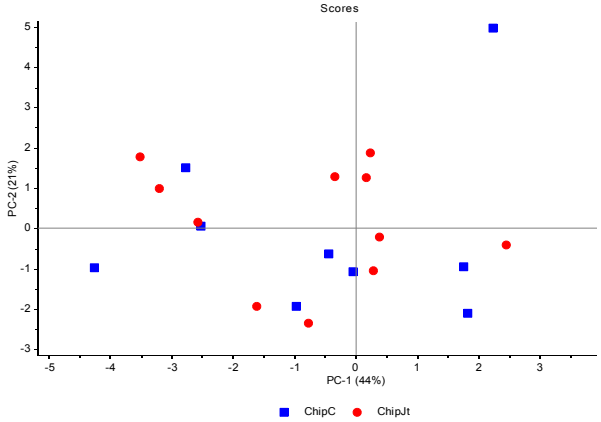

Optimal number of components	Five	Optimal number of components	Eight
Explained variance with optimal number of components			
Calibration (%)	96.0	Calibration (%)	90.1
Validation (%)	92.5	Validation (%)	73.3
Explained variance with 20 components			
Calibration (%)	99.9	Calibration (%)	99.5
Validation (%)	94.6	Validation (%)	78.4

Day 21

Neat synovial fluid

Scores plot of first and second PCA components following outlier removal

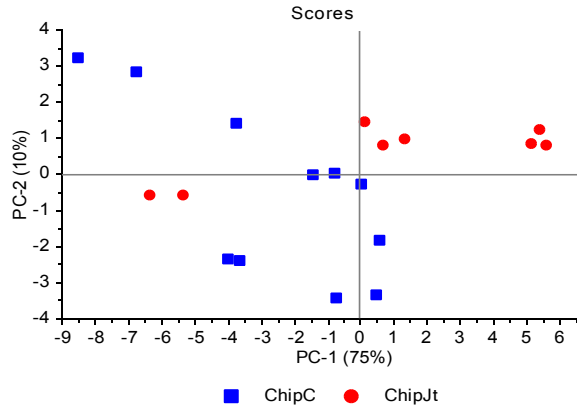

Supernatant of processed synovial fluid

Scores plot of first and second PCA components following outlier removal

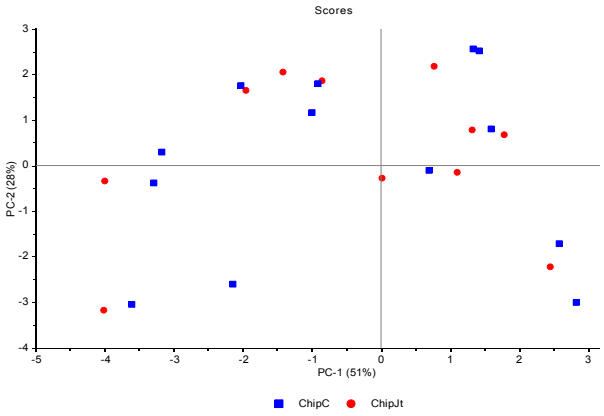

Optimal number of components	Four	Optimal number of components	Six
Explained variance with optimal number of components			
Calibration (%)	94.0	Calibration (%)	91.3
Validation (%)	90.4	Validation (%)	84.5
Explained variance with 20 components (19 only)			
Calibration (%)	99.8	Calibration (%)	98.9
Validation (%)	93.4	Validation (%)	87.5

Day 28

Neat synovial fluid

Scores plot of first and second PCA components following outlier removal

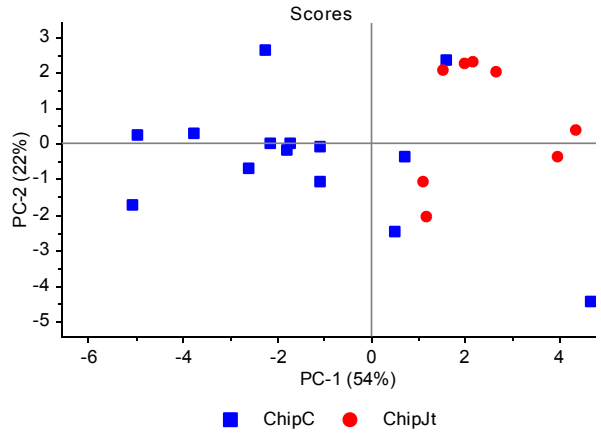

Supernatant of processed synovial fluid

Scores plot of first and second PCA components following outlier removal

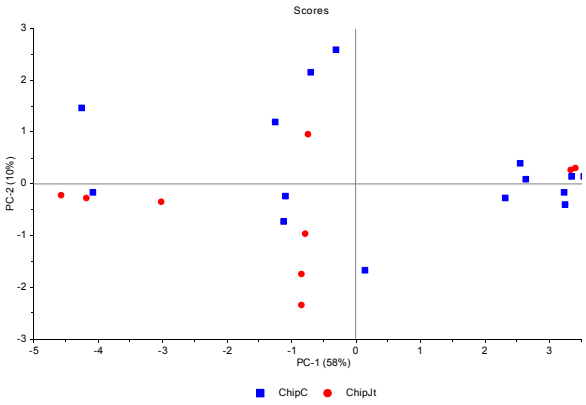

Optimal number of components	Five	Optimal number of components	Four
Explained variance with optimal number of components			
Calibration (%)	89.8	Calibration (%)	78.2
Validation (%)	80.6	Validation (%)	66.4
Explained variance with 20 components			
Calibration (%)	99.8	Calibration (%)	98.7
Validation (%)	84.9	Validation (%)	73.8

Day 35

Neat synovial fluid

Scores plot of first and second PCA components following outlier removal

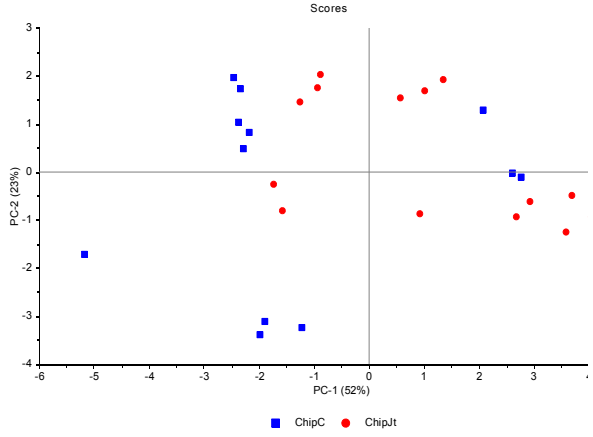

Supernatant of processed synovial fluid

Scores plot of first and second PCA components following outlier removal

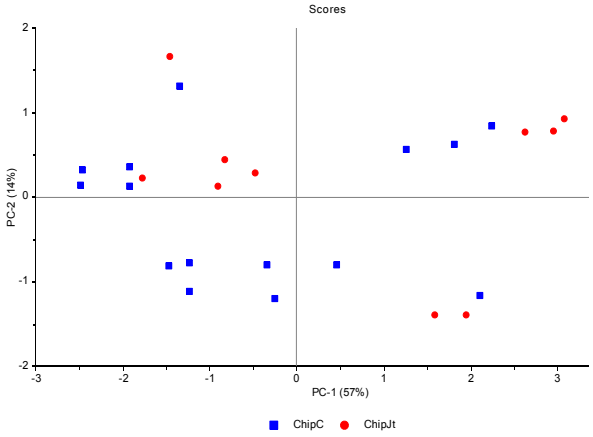

Optimal number of components	Six	Optimal number of components	Five
Explained variance with optimal number of components			
Calibration (%)	93.3	Calibration (%)	85.6
Validation (%)	84.5	Validation (%)	76.5
Explained variance with 20 components			
Calibration (%)	99.3	Calibration (%)	98.8
Validation (%)	89.3	Validation (%)	81.3

Day 42

Neat synovial fluid

Scores plot of first and second PCA components following outlier removal

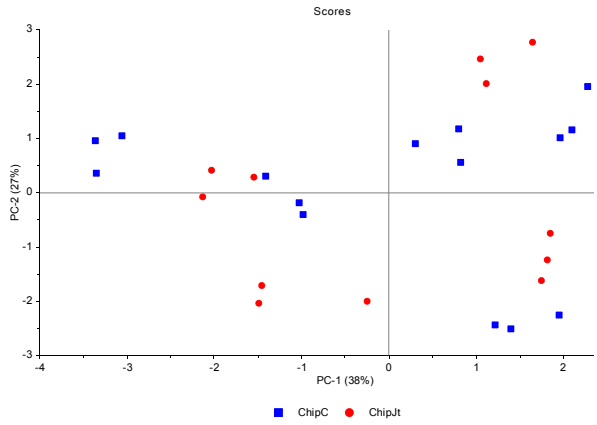

Supernatant of processed synovial fluid

Scores plot of first and second PCA components following outlier removal

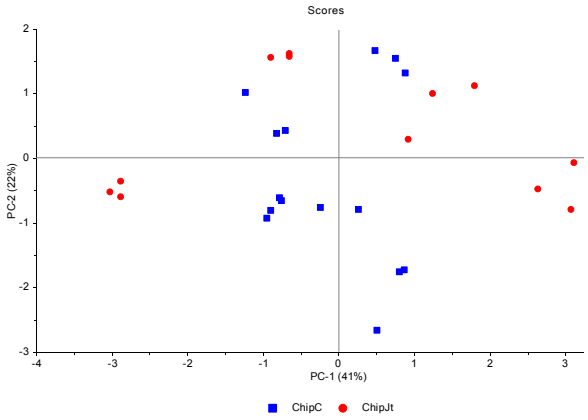

Optimal number of components	Seven	Optimal number of components	Seven
Explained variance with optimal number of components			
Calibration (%)	90.4	Calibration (%)	84.3
Validation (%)	81.5	Validation (%)	70.1
Explained variance with 20 components			
Calibration (%)	98.7	Calibration (%)	97.6
Validation (%)	84.9	Validation (%)	74.7

Day 49

Neat synovial fluid

Scores plot of first and second PCA components following outlier removal

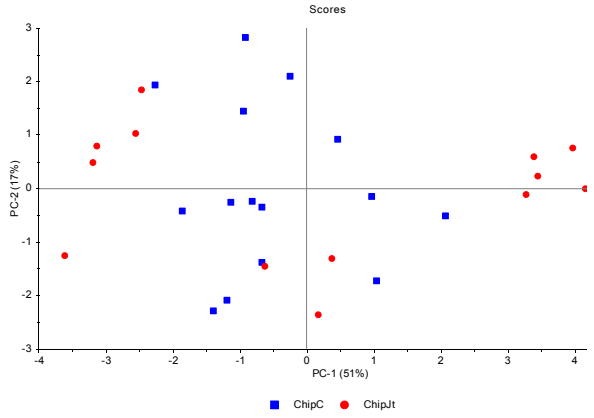

Supernatant of processed synovial fluid

Scores plot of first and second PCA components following outlier removal

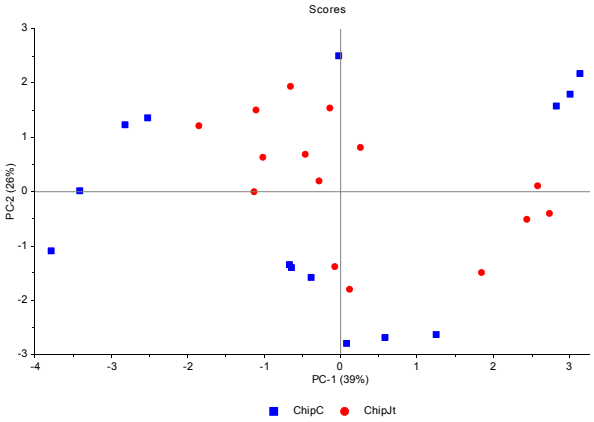

Optimal number of components	Five	Optimal number of components	Five
Explained variance with optimal number of components			
Calibration (%)	85.4	Calibration (%)	85.2
Validation (%)	76.9	Validation (%)	77.5
Explained variance with 20 components			
Calibration (%)	97.8	Calibration (%)	98.0
Validation (%)	81.8	Validation (%)	82.0

Day 56

Neat synovial fluid

Scores plot of first and second PCA components following outlier removal

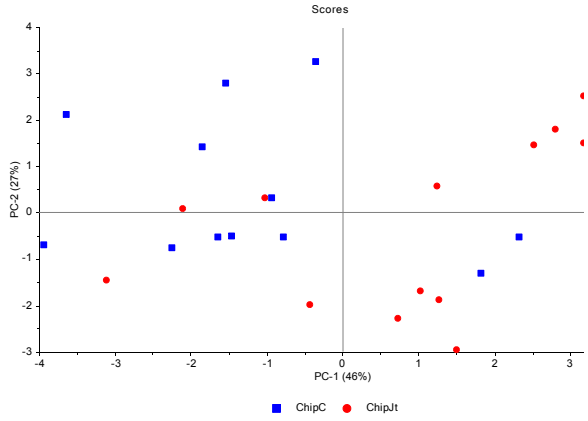

Supernatant of processed synovial fluid

Scores plot of first and second PCA components following outlier removal

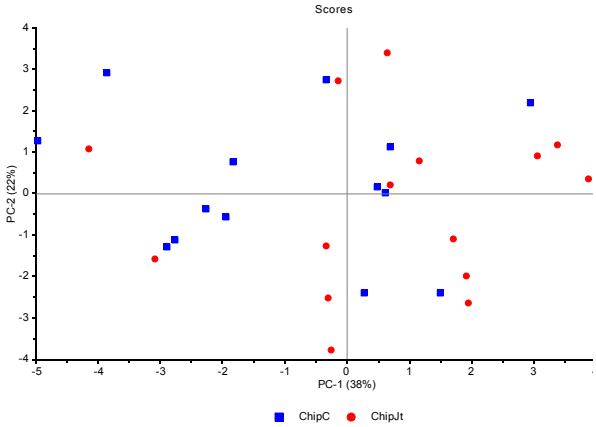

Optimal number of components	Four	Optimal number of components	Six
Explained variance with optimal number of components			
Calibration (%)	86.0	Calibration (%)	85.1
Validation (%)	79.5	Validation (%)	74.9
Explained variance with 20 components			
Calibration (%)	98.9	Calibration (%)	97.4
Validation (%)	84.8	Validation (%)	80.8

Day 63

Neat synovial fluid

Scores plot of first and second PCA components following outlier removal

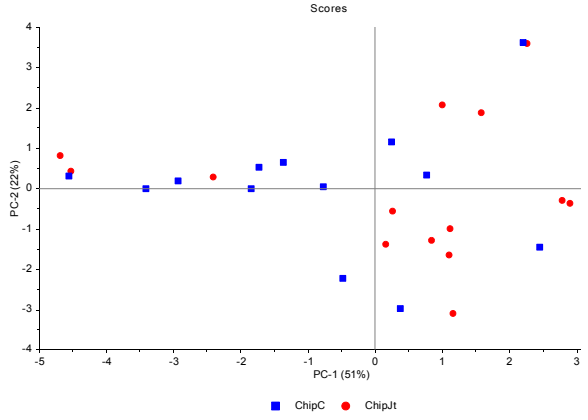

Supernatant of processed synovial fluid

Scores plot of first and second PCA components following outlier removal

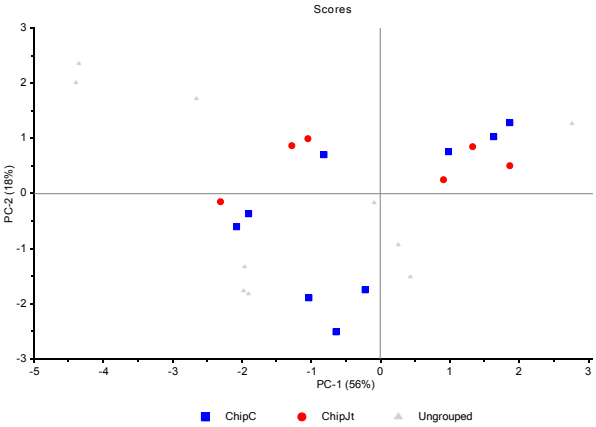

Optimal number of components	Five	Optimal number of components	Four
Explained variance with optimal number of components			
Calibration (%)	86.9	Calibration (%)	84.3
Validation (%)	80.0	Validation (%)	78.8
Explained variance with 20 components			
Calibration (%)	98.3	Calibration (%)	97.8
Validation (%)	85.5	Validation (%)	84.2

Appendix 2. Chip vs. Sham

Results – PCA based classification of synovial fluid samples from horses with an experimentally induced radiocarpal bone fracture versus horses with sham operated radiocarpal joints

Day 0 (preoperative)

Neat synovial fluid

Scores plot of first and second PCA components following outlier removal

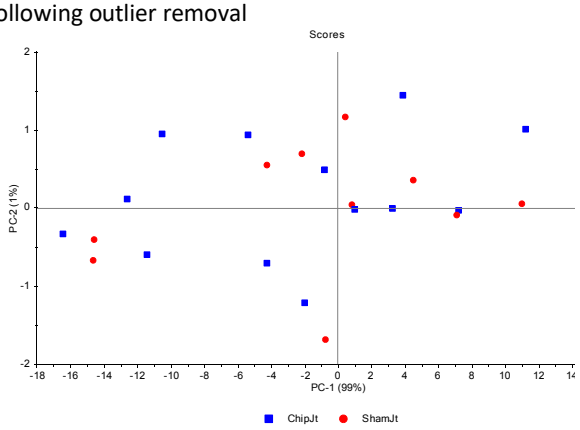

Supernatant of processed synovial fluid

Scores plot of first and second PCA components following outlier removal

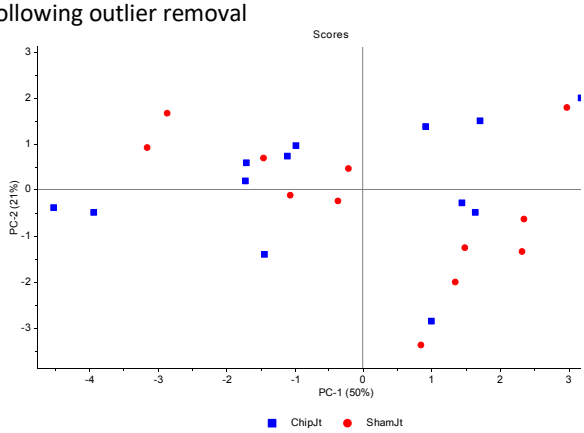

Optimal number of components	One	Optimal number of components	Six
Explained variance with optimal number of components			
Calibration (%)	98.9	Calibration (%)	91.0
Validation (%)	98.8	Validation (%)	83.4
Explained variance with 20 components			
Calibration (%)	100	Calibration (%)	99.0
Validation (%)	100	Validation (%)	86.1

Day 7

Neat synovial fluid

Scores plot of first and second PCA components following outlier removal

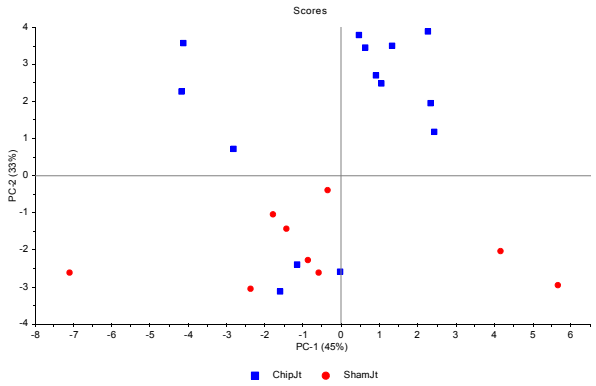

Supernatant of processed synovial fluid

Scores plot of first and second PCA components following outlier removal

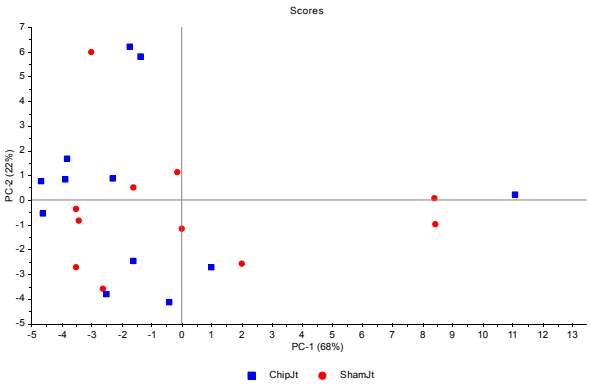

Optimal number of components	Six	Optimal number of components	Four
Explained variance with optimal number of components			
Calibration (%)	94.4	Calibration (%)	95.5
Validation (%)	87.3	Validation (%)	92.3
Explained variance with 20 components			
Calibration (%)	99.7	Calibration (%)	99.8
Validation (%)	90.8	Validation (%)	94.8

Day 14

Neat synovial fluid

Scores plot of first and second PCA components following outlier removal

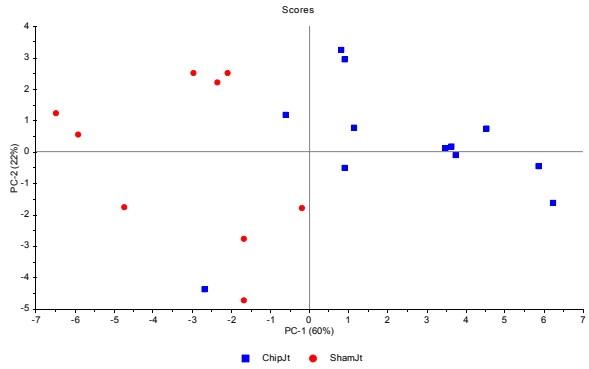

Optimal number of components Six

Explained variance with optimal number of components

Calibration (%)	97.0
Validation (%)	92.8

Explained variance with 20 components (19 cpts)

Calibration (%)	99.9
Validation (%)	94.7

Supernatant of processed synovial fluid

Scores plot of first and second PCA components following outlier removal

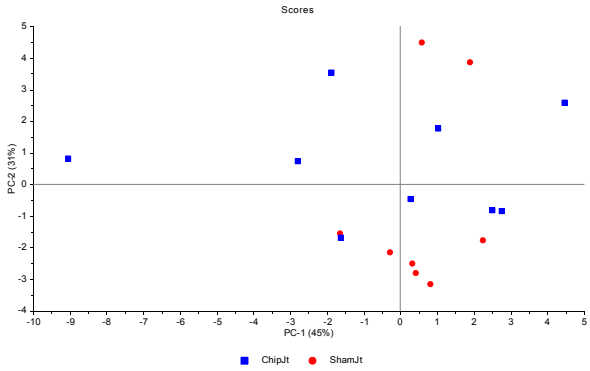

Optimal number of components Four

(15 components only due to exclusion of outliers)

Calibration (%)	86.5
Validation (%)	72.8
Calibration (%)	99.6
Validation (%)	77.6

Day 21

Neat synovial fluid

Scores plot of first and second PCA components following outlier removal

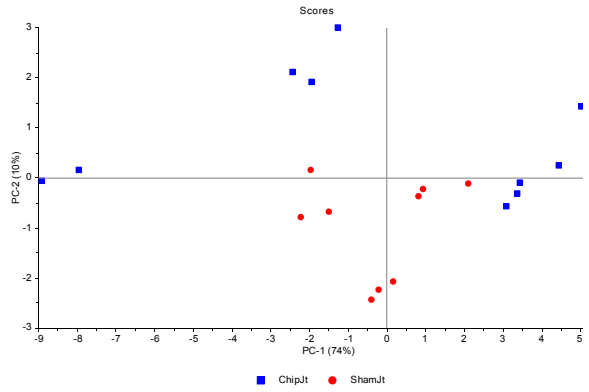

Optimal number of components Six

Explained variance with optimal number of components

Calibration (%)	94.8
Validation (%)	88.8

Explained variance with 20 components (18 PCA cpts)

Calibration (%)	99.8
Validation (%)	91.2

Supernatant of processed synovial fluid

Scores plot of first and second PCA components following outlier removal

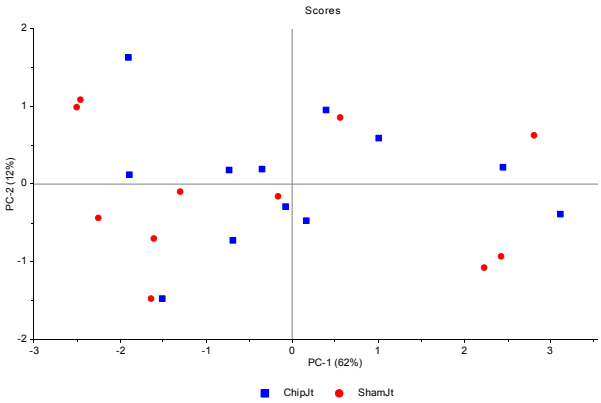

Optimal number of components Six

Calibration (%)	86.8
Validation (%)	75.6
Calibration (%)	99.0
Validation (%)	79.8

Day 28

Neat synovial fluid

Scores plot of first and second PCA components following outlier removal

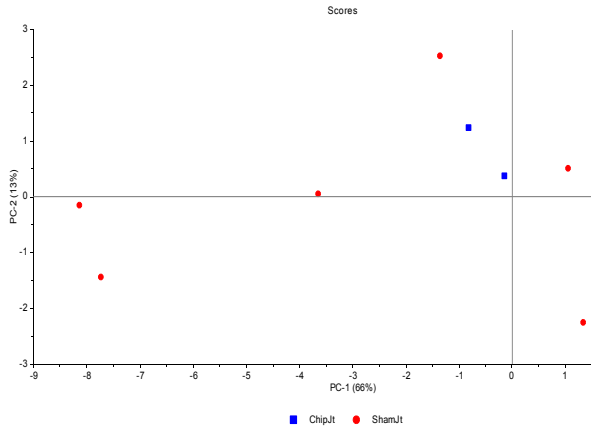

Supernatant of processed synovial fluid

Scores plot of first and second PCA components following outlier removal

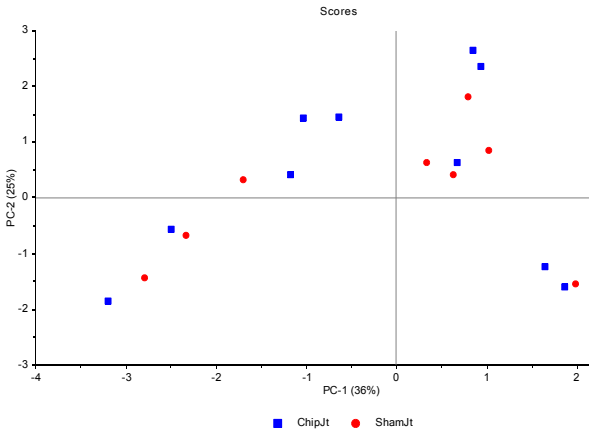

Optimal number of components	Three	Optimal number of components	Four
Explained variance with optimal number of components			
Calibration (%)	88.8	Calibration (%)	73.6
Validation (%)	85.5	Validation (%)	57.3
Explained variance with 20 components (15 cpts)		(18 components only due to exclusion of outliers)	
Calibration (%)	99.8	Calibration (%)	99.3
Validation (%)	86.3	Validation (%)	64.5

Day 35

Neat synovial fluid

Scores plot of first and second PCA components following outlier removal

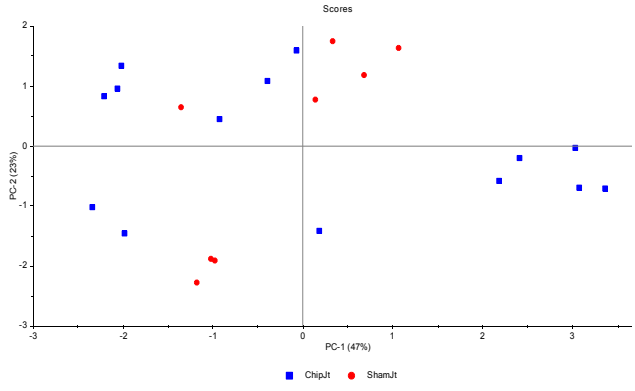

Supernatant of processed synovial fluid

Scores plot of first and second PCA components following outlier removal

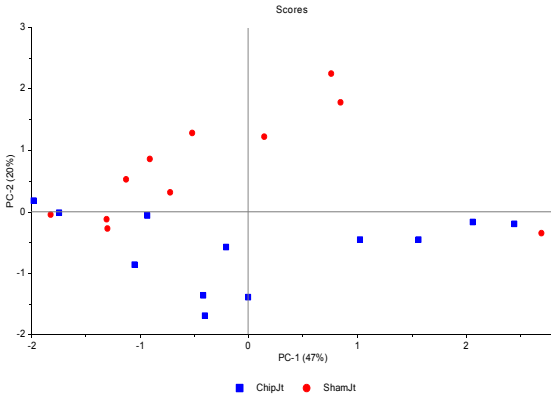

Optimal number of components	Eight	Optimal number of components	Five
Explained variance with optimal number of components			
Calibration (%)	92.5	Calibration (%)	81.6
Validation (%)	80.5	Validation (%)	69.5
Explained variance with 20 components			
Calibration (%)	99.8	Calibration (%)	98.9
Validation (%)	83.5	Validation (%)	75.8

Day 42

Neat synovial fluid

Scores plot of first and second PCA components following outlier removal

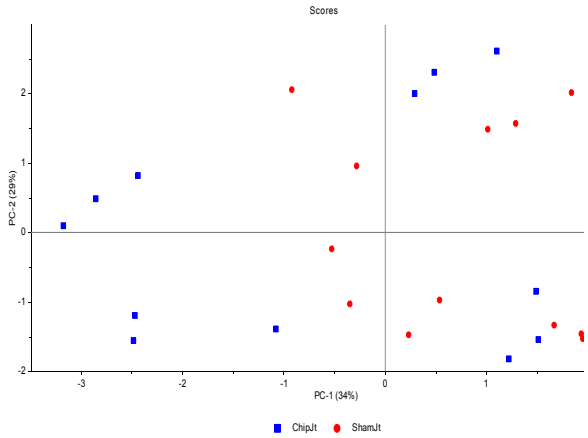

Supernatant of processed synovial fluid

Scores plot of first and second PCA components following outlier removal

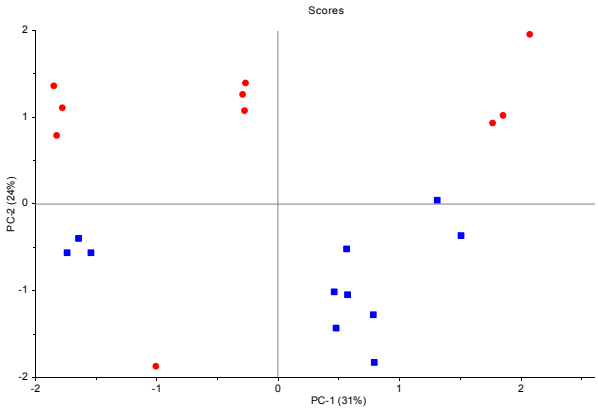

Optimal number of components	Eleven	Optimal number of components	Five
Explained variance with optimal number of components			
Calibration (%)	94.8	Calibration (%)	80.9
Validation (%)	79.9	Validation (%)	59.2
Explained variance with 20 components		(19 components only due to exclusion of outliers)	
Calibration (%)	99.4	Calibration (%)	99.5
Validation (%)	82.3	Validation (%)	66.1

Day 49

Neat synovial fluid

Scores plot of first and second PCA components following outlier removal

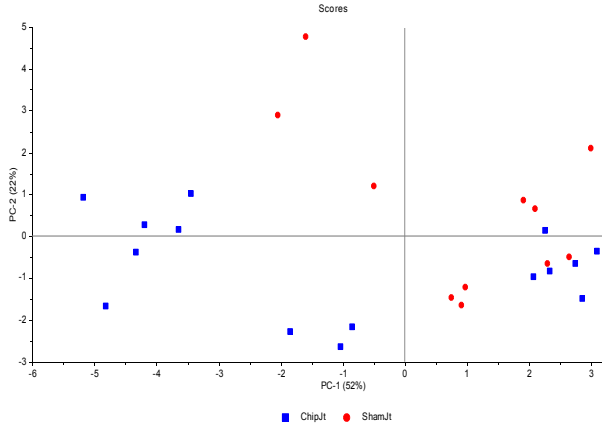

Supernatant of processed synovial fluid

Scores plot of first and second PCA components following outlier removal

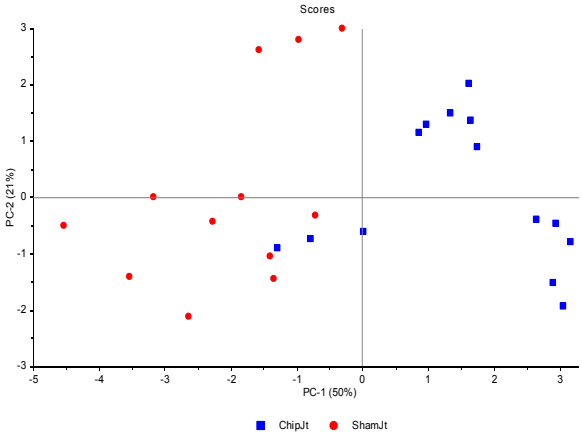

Optimal number of components	Five	Optimal number of components	Five
Explained variance with optimal number of components			
Calibration (%)	88.5	Calibration (%)	86.6
Validation (%)	81.3	Validation (%)	78.9
Explained variance with 20 components			
Calibration (%)	98.7	Calibration (%)	98.6
Validation (%)	85.4	Validation (%)	83.7

Day 56

Neat synovial fluid

Scores plot of first and second PCA components following outlier removal

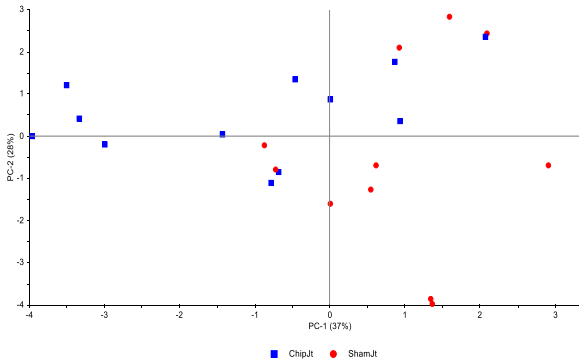

Supernatant of processed synovial fluid

Scores plot of first and second PCA components following outlier removal

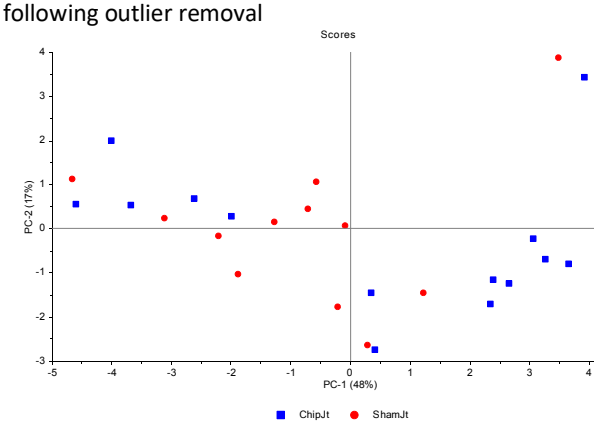

Optimal number of components	Four	Optimal number of components	Five
Explained variance with optimal number of components			
Calibration (%)	85.7	Calibration (%)	85.6
Validation (%)	78.4	Validation (%)	77.3
Explained variance with 20 components			
Calibration (%)	99.4	Calibration (%)	98.3
Validation (%)	85.1	Validation (%)	83.2

Day 63

Neat synovial fluid

Scores plot of first and second PCA components following outlier removal

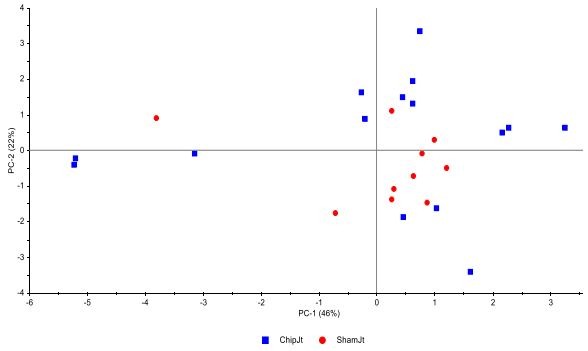

Supernatant of processed synovial fluid

Scores plot of first and second PCA components following outlier removal

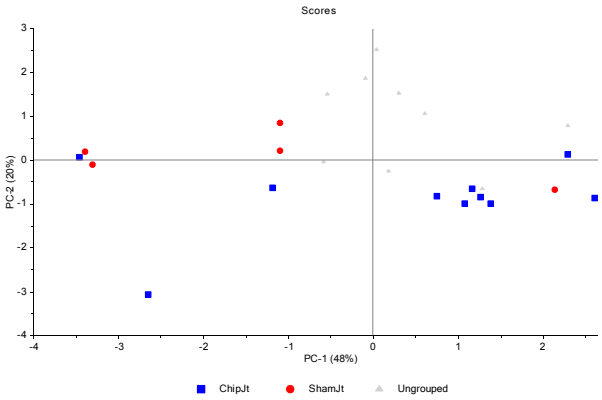

Optimal number of components	Five	Optimal number of components	Five
Explained variance with optimal number of components			
Calibration (%)	86.3	Calibration (%)	82.1
Validation (%)	76.1	Validation (%)	69.5
Explained variance with 20 components			
Calibration (%)	99.0	Calibration (%)	99.0
Validation (%)	82.3	Validation (%)	77.1